Zeitschrift für Physikalische Chemie, **214**, 11, 1479−1500 (2000)
© by Oldenbourg Wissenschaftsverlag, München

The Heterogeneous Kinetics of the Reactions $ClONO_2$ + HX/ice (X = Br, I), $BrONO_2$ + HI/ice and the Reactivity of the Interhalogens BrCl, ICl and IBr with HX/ice (X = Cl, Br, I) in the Temperature Range 180 to 205 K

By A. Allanic[1], R. Oppliger[2], H. van den Bergh and M. J. Rossi[3,*]

[1] Center for Research into Atmospheric Chemistry, University College Cork, Cork, Ireland
[2] Iware SA, Avenue de La Gottaz 34, CH-1110 Morges, Switzerland
[3] Laboratoire de Pollution Atmosphérique et Sol (LPAS), Ecole Polytechnique Fédérale de Lausanne (EPFL), CH-1015 Lausanne, Switzerland

Dedicated to Prof. Dr. Dr. h. c. mult. Jürgen Troe on the occasion of his 60th birthday

(Received May 30, 2000; accepted July 11, 2000)

Heterogeneous Chemical Kinetics / Atmospheric Processes / Vapor-Phase Condensed Ice / Ice Substrates / $ClONO_2$ / $BrONO_2$ / Interhalogen Compounds

The kinetics and mechanism of the title heterogeneous halogen exchange reactions of potential atmospheric importance have been studied under molecular flow conditions in a FEP Teflon-coated Knudsen flow reactor on HX (X = Cl, Br, I) − doped ice condensed from the vapor phase under conditions of several formal monolayers of HX coverage at approximately 200 K. In addition, the halogen exchange reactions involving the expected primary reaction products BrCl, ICl and IBr of the above mixed anhydrides with HX-doped ice have been studied at 200 K as well. The uptake coefficient γ for the heterogeneous reaction $ClONO_2$ + HBr on ice is 0.56 ± 0.11 and Cl_2 and Br_2 are formed in yields of 100% and 66 to 80%, respectively, in the range 180 to 200 K. The γ value for the reaction $ClONO_2$ + HI on ice is 0.30 ± 0.02 at 200 K with Cl_2 being the main product appearing after an induction time. The primary product ICl is formed at the same time as Cl_2 whereas HOCl appears at a later time under conditions of waning HI supply. The γ value for the reaction $BrONO_2$ + HI on ice is 0.40 ± 0.02 at 200 K with Br_2 being the main product observed after a short delay. The primary product IBr is observed without delay, whereas HOBr is observed at a later time once HBr has reacted. The mechanism

* Correspondence author. E-mail: michel.rossi@epfl.ch

Brought to you by | New York University Bobst Library Technical Services
Authenticated
Download Date | 7/25/15 6:50 AM

of the reactions of the interhalogens BrCl, ICl and IBr with HX on ice at 200 K involves the formation of trihalide ions at the ice interface which is consistent with the observed significant negative temperature dependence for the reaction ICl + HBr on ice in the range 180 to 205 K as well as for the reaction BrCl + HBr between 190 and 200 K. The uptake coefficient γ for each of the interhalogens increases from ice to HI-doped ice in the order of increasing molecular weight of HX with the exception of ICl, whose γ attains a limiting value of $\gamma = 0.32 \pm 0.05$. A halogen exchange reaction on ice has been observed in cases where the most stable hydrohalic acid could be formed: HCl > HBr > HI. A propensity for the formation of the homonuclear halogen molecule in the reactions of halogen nitrates with HX-doped ice has been explained by the occurrence of fast secondary reactions of the primary interhalogen product at the HX/ice interface.

1. Introduction

The importance of chlorine and bromine in catalytic cycles of stratospheric ozone destruction and their role in heterogeneous reactions has been studied extensively [1−3]. One of the most important heterogeneous reactions is the prototypical reaction (1) in which two inactive reservoir molecules combine in an efficient way to generate Cl_2 which will rapidly liberate two Cl atoms upon photolysis.

$$ClONO_2 + HCl \rightarrow Cl_2 + HNO_3 . \quad (1)$$

It has been shown that reaction (1) occurs in a direct way on ice and other frozen surfaces without going through hydrolysis of $ClONO_2$ to result in HOCl which itself reacts with HCl in a rapid heterogeneous reaction [4]. This direct mechanism is thought to be key to the importance of reaction (1) in ozone depletion scenarios. Halogen as well as halogen-NO_x mixed anhydrides may perhaps be important in the ozone chemistry of the Arctic troposphere where even higher ozone destruction rates compared to the stratosphere have been recorded [5]. In particular, bromine-containing molecules such as BrO and HOBr seem to be involved in autocatalytic halogen activation reactions leading to a rapid increase of BrO_x (= BrO + HOBr + …) concentration. Bromine monoxide BrO is, in addition to HBr [6], among the most important active bromine compounds which has been observed both in the stratosphere [7, 8] as well as in the troposphere [9]. Under certain conditions the measured local tropospheric concentrations of BrO can by far exceed the stratospheric concentrations, both in the Arctic [10] as well as in the midlatitude troposphere [11]. In the presence of NO_x bromine oxide recombines to $BrONO_2$ which has not been observed to date, neither in the stratosphere nor in the troposphere. However, BrO concentration fields which are increasingly being studied using both remote sensing techniques such as satellite imagery [10] as well as local measurement methods such as DOAS [11] in conjunction with known NO_x concentration fields should result in reliable concentrations of $BrONO_2$ whose photolytic [12] and heterogeneous reactivity [13, 14] has been well documented.

Brought to you by | New York University Bobst Library Technical Services
Authenticated
Download Date | 7/25/15 6:50 AM

Although it has long been thought that iodine only affected the surface ozone budget [15−17], new scenarios have recently emerged which suggest that iodine could potentially play a non-negligible part in ozone destruction also at higher altitudes [18, 19]. The postulated photooxidation of biogenic iodo-carbons which accounts for much of the iodine source in the atmosphere leads to two major forms of inorganic reservoir compounds of iodine in the upper troposphere, namely HOI and HI [19, 20]. Only a few laboratory investigations have been conducted this far to study the heterogeneous behavior of these compounds [21, 22] and to address the window of uncertainty provided by this missing chemistry in numerical models [18, 19].

HI is photolytically more stable than HOI and the reaction with OH radical is the main gas-phase sink for HI throughout the atmosphere [23]. In addition, wash-out processes will also remove a significant fraction of HI. However, in the upper troposphere heterogeneous losses at the surface of aerosols and ice particles present in high altitude cirrus clouds could actually amount to a recycling of iodine via interhalogen surface reactions such as those presented in this work. Akin to what has been described for chlorine and bromine [24], the coupling of iodine chemistry with that of chlorine or bromine through heterogeneous reactions like reaction (2) could increase the fraction of active forms of halogen species at these altitudes, in turn affecting the ozone budget.

$$XONO_2 + HY \rightarrow XY + HNO_3 \quad (X = Cl, Br; Y = Cl, Br, I)\,. \qquad (2)$$

This mixed-halogen heterogeneous chemistry involves reservoir species like $XONO_2$ and HOX (X = Cl, Br) reacting with HY (Y = Cl, Br, I). The hydrolysis of $ClONO_2$ and $BrONO_2$ on ice is now well documented and experimental studies have shown that both strongly interact with water ice [4, 13, 14, 25]. Recent *ab initio* calculations [26] have concluded that $ClONO_2$ spontaneously reacts with ice, overcoming the weak nucleophilicity of the pure water interface towards the chlorine atom of $ClONO_2$ through partial polarization of the Cl−O bond upon adsorption. The presence of hydrochloric acid increases the rate of reaction (2) for both clorine and bromine nitrate [4, 13, 14, 25]. The electrolytic dissociation of HCl at the interface provides a strong nucleophile (Cl^-) which allows for a direct, facile reaction with $XONO_2$. Similar mechanistic details and particularly the influence of ionized HY (Y = Br, I) at the ice interface on the rate of reaction (2) remains to be studied for the case of $BrONO_2$.

In this paper we report mechanistic aspects of effective bimolecular reactions of $ClONO_2$ and $BrONO_2$ with HCl and HBr adsorbed on ice both as far as the uptake coefficient as well as the nature of the reaction products are concerned. It is apparent that in most cases the observed products are not the expected primary products owing to fast secondary reactions of the primary interhalogen compounds whose reactivity is studied separately in the last section. We point out that the heterogeneous reactions of the inter-

Brought to you by | New York University Bobst Library Technical Services
Authenticated
Download Date | 7/25/15 6:50 AM

halogens YZ with HX (X = Cl, Br, I) are controlled by complex formation of the type XYZ^- which has been used to interpret the interaction of gas phase molecular chlorine and bromine with solutions containing Br^- and I^- at ambient temperature [27]. This complex formation at the interface is a useful concept to understand surface-catalyzed interfacial reactions on solid surfaces as opposed to the conceptual framework which treats heterogeneous reactions as condensed phase reactions of dissolved gas molecules [28].

2. Experimental setup

The kinetic studies of the heterogeneous chemistry have been performed using a low-pressure reactor (Knudsen cell) configured as a flowing gas experiment. The reactor is mounted on a differentially pumped vacuum chamber equipped with a quadrupole mass spectrometer which samples the molecules effusing from the reactor as an effusive molecular beam. The details of the experimental set-up have been discussed previously [29]. Briefly, we have performed the experiments in the molecular flow regime inside a two-chamber Teflon coated reactor which allowed us to isolate the sample surface located in the sample chamber from the gas flowing through the reference chamber. The experiment is essentially a relative rate experiment conducted, on the one hand, with the sample chamber open and, on the other hand, with the sample chamber closed. The measured relative rate constants are put on an absolute basis using experimentally measured escape rate constants for the gas of interest. The escape aperture and thus the residence time of the average molecule in the gas phase is varied by changing the size of the orifice. This is achieved by fitting a plunger-mounted plate containing several orifices of different diameter onto the base plate containing the largest aperture. Both a change of the diameter of the escape orifice as well as a change in the flow rate of the gas into the reactor over a range of almost three orders of magnitude (3.0×10^{10} to 2.0×10^{13} molecule cm^{-3}) affords the necessary variation of pressure and lifetime required to study the mechanism of the heterogeneous reaction of interest. The knowledge of the mechanism allows us to extrapolate the kinetic results to concentrations encountered in the stratosphere which cannot yet be experimentally accessed.

The characteristic parameters of the Knudsen reactor used in this study are displayed in Table 1 together with the range of variation of the experimental variables. The molecular flow regime that prevails in our reactor allows us to calculate the gas-wall collision frequency ω_v using the geometry of the reactor and the gas properties. This frequency is given by $\omega_v = (\langle c\rangle/4\ V)A_v$ where $\langle c\rangle$ is the average molecular velocity of the gas and V and A_v are the volume and the internal surface of the Knudsen cell,

Brought to you by | New York University Bobst Library Technical Services
Authenticated
Download Date | 7/25/15 6:50 AM

Table 1. Characteristic parameters of the Knudsen flow reactors used in this study. T = 300 K gas phase temperature; F^i_M: Flow rate of the species of molar mass M into the reactor.

Definition	Orifice diameter	Value
Reactor volume, V		1830 (cm^3)
Sample surface area, A_s		17 (cm^2)
Escape rate constant, k_{esc}	14 mm	1.77 $(T/M)^{0.5}$ (s^{-1})
	8 mm	0.58 $(T/M)^{0.5}$ (s^{-1})
	4 mm	0.14 $(T/M)^{0.5}$ (s^{-1})
Gas number density, N		F^i_M/Vk_{esc}) (molecule cm^{-3})
Collision frequency, ω_s with A_s		34.7 $(T/M)^{0.5}$ (s^{-1})

respectively. By using A_s, the sample surface, or A_h, the area of the escape orifice for A_v in this formula we may calculate the gas-sample collision frequency ω_s and the escape rate constant k_{esc} for molecular effusion out of the reactor. The first order heterogeneous rate constant k_{het} is given by $k_{het} = k_{esc}(I_0-I)/I$ where I_0 and I are mass spectrometric (MS) intensities in the presence and absence of the sample, respectively. The reactive or non-reactive uptake coefficient γ is determined from the measured rate constant k_{het} divided by the calculated collision frequency ω_s of the average molecule with the substrate surface, $\gamma = k_{het}/\omega_s$. The initial uptake coefficient γ_0 is calculated at time zero or very close to it when the surface coverage is zero. The gas number density or concentration N may be calculated using $N = F^i_M/V \cdot k_{esc}$, with F^i_M being the measured flow rate into the Knudsen cell of species of molar mass M.

Because molecular diffusion in the reactor proves to be rate-limiting under certain conditions, discrepancies between the measured and calculated values of k_{esc} and ω have been observed. These discrepancies were largest for the largest escape orifice of 14 mm diameter [29, 30]. The values and expressions listed in Table 1 are based on experimental observations of k_{esc}. Similar molecular diffusion limitations affecting large uptake rates measured in the present flow reactor were also reported by these authors and the correction recommended by Fenter *et al.* [30] was systematically applied to measured uptake coefficients which were in excess of 0.4. All values for γ and γ_0 reported in the following sections are therefore considered to be accurate.

For the preparation of the low temperature ice substrates we used a low temperature sample support described in detail elsewhere [4]. Briefly, the temperature of a copper dish is regulated to ± 1 K using a PID temperature controller by alternating periods of cooling and heating. The absolute temperature scale has been calibrated against the known vapor pressure of H_2O over ice monitored at m/e18. The ice samples were prepared by admitting

Brought to you by | New York University Bobst Library Technical Services
Authenticated
Download Date | 7/25/15 6:50 AM

a high H_2O vapor flow rate of approximately 1×10^{19} molecule s^{-1} into the reactor once the sample dish had reached the target temperature of the experiment of approximately 190 K. Exposure of this flow to the cold copper substrate for approximately five minutes resulted in a thick vapor-condensed ice film of up to 1.5×10^5 monolayers corresponding to a thickness of approximately 75 μm when the bulk density of ice was used in the calculation. This film was kept in thermodynamic equilibrium by adjusting an external water flow so as to cancel evaporation and condensation rates, thus resulting in no net water vapor uptake.

When referring to doped ice in the next sections we mean an ice sample that has been exposed to a high flow of HX (X = Cl, Br, I) on the order of a few 10^{15} molecule s^{-1}, for a time long enough depending on the uptake coefficient [21] to ensure the adsorption of about ten formal monolayers of HX at the interface. An exception is the study of the reaction $ClONO_2$ + HBr where approximately two formal monolayers of HBr have been deposited on ice condensed from the vapor phase prior to the uptake experiment. The loss of HCl by evaporation was strictly controlled by quantitatively monitoring the amount of thermally desorbing HCl from doped samples following an experiment. Neither HBr nor HI supported a partial pressure over ice at the temperatures of interest [21]. At the end of each experiment the HY-doped ice was heated so that adsorbed, potential reaction products together with the unreacted fraction of HY could be thermally desorbed and monitored using MS.

Reactant preparation

$ClONO_2$ was synthesized by reacting Cl_2O with excess N_2O_5 at low temperature following the procedure described by Timonen *et al.* [31]. The main impurity in the sample was Cl_2 the amount of which was minimized through repeated freeze-pump-thaw cycles and passivation of the storage volume wall prior to experiments. $BrONO_2$ was produced according to the procedure described by Wilson and Christe [32] by mixing $ClONO_2$ and Br_2. The main observed contaminants were Br_2 and BrCl whose amounts were kept to a minimum by careful distillation and storage volume wall passivation. HCl and HI were produced in the laboratory, the former by reacting H_2SO_4 with dry NaCl, the latter by letting react I_2 on amorphous (red) phosphorous in the presence of water. HBr was sampled from a lecture bottle (Messer-Griesheim GmbH) and subsequently purified from H_2 and Br_2 contamination by distilling it from the HBr/Br_2 mixture at low temperature. BrCl was produced by mixing gaseous Br_2 with an excess of Cl_2 following the prescription given by Stull *et al.* [33]. Once equilibrium had been obtained excess Cl_2 was removed by vacuum distillation at 200 K. Gaseous ICl and IBr were collected from the vapor pressure established

Brought to you by | New York University Bobst Library Technical Services
Authenticated
Download Date | 7/25/15 6:50 AM

Table 2. Main results of continuous flow experiments for the heterogeneous reaction of $ClONO_2$ on ice condensed from the vapor phase and doped with HBr at 180 and 200 K.

Temperature [K]	Aperture diameter [mm]	Uptake coefficient γ	Cl_2 yield [%]	Br_2 yield [%]
180	4	0.66	114	111
180	8	0.48	105	115
180	8	0.61	109	43
180	8	0.70	100	84
		average yield	104.7±4.5	80.7±36.1
180	14	0.50	100	63
180	14	0.54	93	85
180	14	0.76	90	95
		average yield	94.3±5.1	81.0±16.4
200	4	0.40	111	82
200	8	0.55	–	88
200	8	0.56	99	50
200	8	0.42	85	59
		average yield	92.0±9.9	65.7±19.8
200	14	0.68	–	80
200	14	0.51	70	47
200	14	0.46	107	70
		average yield	88.5±26.2	65.7±16.9

over their respective solid, crystalline forms which were kept in evacuated traps. Crystalline ICl (Fluka pract. ≈ 97%) and IBr (Fluka pract. ≈ 96%) are commercially available samples.

3. Results and discussion

A. $ClONO_2$ + HBr/ice

The heterogeneous reaction of $ClONO_2$ on ice doped with HBr has been measured in the temperature range 180−200 K at various concentrations of $ClONO_2$. The uptake coefficient γ has been measured in continuous flow experiments by monitoring the disappearance of $ClONO_2$ from the gas phase at m/e 46 and the results are displayed in Table 2: γ is invariant to the change in escape orifice diameter and thus independent of the partial pressure in the range 180 to 200 K. Under these experimental conditions $ClONO_2$ was the sole contributor to m/e 46 as the reaction product HNO_3 did not desorb from the ice interface at the used temperatures and doses. The experiment has been performed in two steps: at first, the ice sample was exposed for a given amount of time to a high flow rate of HBr which

Brought to you by | New York University Bobst Library Technical Services
Authenticated
Download Date | 7/25/15 6:50 AM

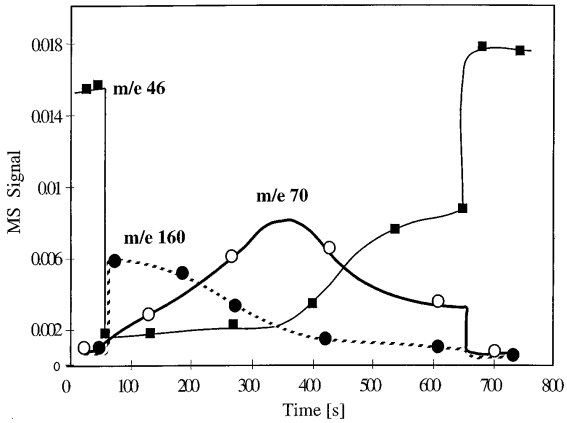

Fig. 1. Continuous flow experiment of $ClONO_2$ on an ice sample condensed from vapor phase H_2O and doped with HBr at 190 K at a gas phase residence time of 3.1 s. $ClONO_2$ is let into the reactor at 10^{14} molecule s^{-1} and monitored at m/e 46 (squares). Br_2 monitored at m/e 160 (full circles) appears promptly and Cl_2 is monitored at m/e 70 (open circles). The start and stop of the uptake experiment is at t = 50 and 640 s, respectively. The lines guide the eye and represent an average through the data points (not shown).

was moniored at m/e 80. This information allows one to determine the quantity of HBr deposited on the ice surface, which amounted to approximately 2 formal monolayers. In the second step $ClONO_2$ was admitted to the flow reactor and the uptake experiment was performed by simultaneously monitoring m/e 46 as a marker for $ClONO_2$ and m/e 160 (Br_2^+) and 70 (Cl_2^+), a typical example of which is displayed in Fig. 1. BrCl, the expected primary reaction product of reaction (3), has not been detected at m/e 114 ($BrCl^+$) at the prevailing sensitivity of the

$$ClONO_2 + HBr \rightarrow BrCl + HNO_3 . \qquad (3)$$

MS, presumably because of the fast secondary reaction of BrCl generated *in situ* with excess HBr. The formation of the observed reaction products Br_2 and Cl_2 could be explained by reaction (4) which will be presented in more detail below and which results in Br_2, followed by reaction (1) which leads to the generation of Cl_2. The high rate of reaction (4) precludes the observation of BrCl as an intermediate because BrCl desorption apparently cannot compete against reaction (4), and only Br_2 is

$$BrCl + HBr \rightarrow Br_2 + HCl \qquad (4, IH3)$$

observed, even at the beginning of the uptake experiment under the present experimental conditions. The rate of formation of Br_2 is largest at the beginning and slows down with time owing to the decreasing concentration of HBr at the interface. Concomitantly with the decrease of the rate of forma-

Brought to you by | New York University Bobst Library Technical Services
Authenticated
Download Date | 7/25/15 6:50 AM

tion of Br_2 an increase in the rate of Cl_2 formation is observed reaching a maximum at t = 350 s (see Fig. 1) once reaction (4) has accumulated a sufficient amount of HCl at the interface such that reaction (1) may occur at its maximum rate. Synchronously with the decrease of the Cl_2 rate of formation at later times the $ClONO_2$ uptake coefficient γ decreases and attains the smaller value of the $ClONO_2$ hydrolysis, reaction (5). Therefore, once all the HBr and HCl at the interface have reacted,

$$ClONO_2 + H_2O \rightarrow HOCl + HNO_3 \quad (5)$$

HOCl monitored at m/e 52 ($HOCl^+$ not shown in Fig. 1) starts to appear in agreement with previous work [4]. Finally, the frozen condensate is slowly warmed up in order to desorb the reaction products that have remained adsorbed during the continuous flow experiment. Beyond 220 K towards higher temperatures HNO_3, HBr and sometimes Br_2 monitored at m/e 46, 80 and 160, respectively, have been detected which enabled us to close the mass balance between $ClONO_2$ consumed and HNO_3 produced.

The values of γ obtained at 180 to 200 K displayed in Table 2 did show neither a temperature nor a flow rate dependence so that the rate law is effectively first order in $ClONO_2$ with an average value of $\gamma = 0.56 \pm 0.11$ in the given temperature range. This value of γ is a factor of two larger than the corresponding value for reaction (1) occurring on ice [34] for similar quantities of adsorbed HX.

An important feature constraining the reaction mechanism is the absolute and relative yield of Cl_2 and Br_2 reflecting the partition between Cl and Br containing compounds resulting from the complex reaction scheme (3), (4) and (1). The absolute yield y_{Cl_2} of Cl_2 and y_{Br_2} of Br_2 are given by the time integral of the instantaneous yields y_{Cl_2} and y_{Br_2} presented in Eqs. (6) and (7) with a

$$y_{Cl_2} = 2\,F^o_{Cl_2}/(F^i_{ClONO_2} - F^o_{ClONO_2}) \quad (6)$$

$$y_{Br_2} = F^o_{Br_2}/(F^i_{ClONO_2} - F^o_{ClONO_2}) \quad (7)$$

typical integration period of 600 s (Fig. 1) which corresponds to the time at which the reaction essentially stops yielding the reaction products Br_2 and Cl_2, even though not all the HBr originally deposited may have reacted. In expressions (6) and (7) F is the flow rate in (F^i) and out (F^o) of the Knudsen flow reactor depending on the superscript i and o, respectively. The stoichiometric factor of 2 in expression (6) takes into account that two molecules of $ClONO_2$ are necessary to form a molecule of Cl_2 whereas only one is required to form Br_2 because one of the bromine atoms stems from HBr present in excess at the interface. Table 2 displays the integrated yields as a function of the residence time of $ClONO_2$ in the Knudsen flow reactor at 180 K and 200 K. It appears that y_{Cl_2} is 100% within experimental uncertainty and independent of the Cl_2 residence time whereas y_{Br_2} is significantly smaller than 100% with respect to Cl_2 thus indicating that Br_2 may be retain-

Brought to you by | New York University Bobst Library Technical Services
Authenticated
Download Date | 7/25/15 6:50 AM

ed to a significant extent by the HBr/ice matrix. This conclusion has been corroborated by independent reference experiments carried out previously [35]. As expected, the absolute Br_2 yield y_{Br_2} decreases with increasing temperature as may be seen in Table 2, namely $y_{Br_2} \approx 80\%$ at 180 K and $y_{Br_2} \approx 66\%$ at 200 K.

In conclusion, it appears that reaction (3) is characterized by a temperature independent uptake coefficient γ larger than the chlorine only system (reaction (1)) and the absence of the expected primary reaction product BrCl. Instead, we observe a definite propensity of the system for the formation of the homonuclear molecular halogen through a complex reaction mechanism comprising three heterogeneous reactions whose rates are comparable to each other. The absolute yield of Cl_2 attains 100% within experimental uncertainty whereas the bromine yield is significantly smaller than 100% owing to interaction of Br_2 with excess HBr on the ice interface resulting in a complex of the type $H^+ \cdots Br_3^-$ in analogy to trihalide ions observed in solution using transient spectroscopy (see below). In addition, it has been recognized recently that not all of the HBr deposited onto ice may be consumable in a given reaction. Examples include the heterogeneous reactions of N_2O_5 + HBr [35] and HONO + HBr on ice [36]. The rate law is of apparent first order in $ClONO_2$ although deviations may perhaps be recognizable at 200 K in the longest residence time Knudsen reactor (see Table 2).

B. $ClONO_2$ + HI/ice

The reaction of interest is displayed in reaction (8) with ICl as the expected primary reaction product:

$$ClONO_2 + HI \rightarrow ICl + HNO_3 . \qquad (8)$$

A typical uptake experiment of $ClONO_2$ on HI doped ice under continuous flow conditions at 200 K is presented in Fig. 2. The uptake of $ClONO_2$ is very fast leading to mean value of $\gamma = 0.30 \pm 0.02$ whose magnitude is within a factor of two of γ obtained in the presence of HBr. The observed reaction products are ICl, Cl_2 and HOCl monitored at m/e 162 (ICl^+), 70 (Cl_2^+) and 52 ($HOCl^+$), respectively, whose relative importance vary with time after the start of the uptake experiment (Fig. 2). The most noteworthy fact is the absence of any gas phase reaction product at the start of the uptake experiment and the significant induction time for the appearance of Cl_2 and ICl. As the supply of HI available at the ice interface is waning, the uptake of $ClONO_2$ slightly decreases together with the formation of Cl_2 at approximately t = 300 s and ICl starts to appear in the gas phase. At t = 550 s the uptake of $ClONO_2$ begins to saturate indicating that the hydrolysis reaction (5) forming HOCl is becoming progressively dominant as was the case for reaction (3) discussed above because reaction (8) is slowing down

Brought to you by | New York University Bobst Library Technical Services
Authenticated
Download Date | 7/25/15 6:50 AM

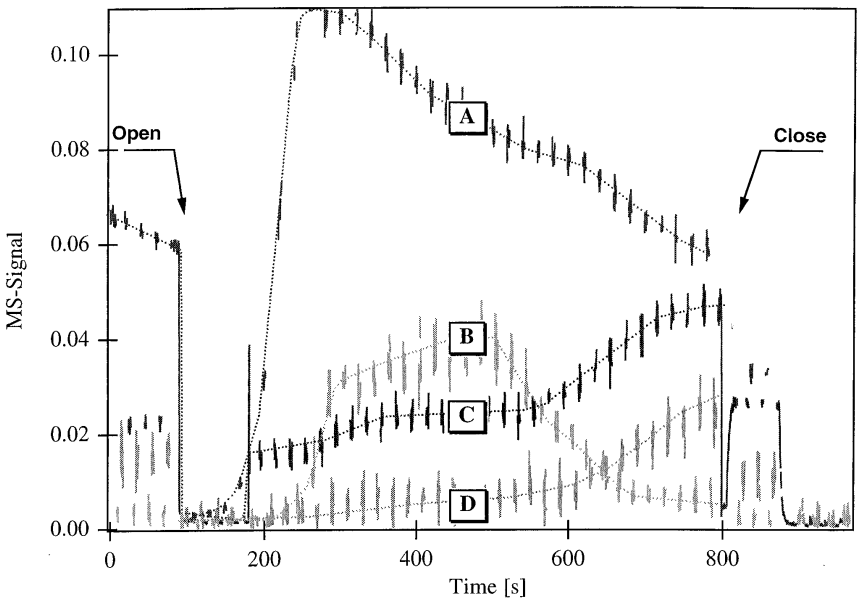

Fig. 2. The interaction of $ClONO_2$ with HI-doped ice condensed from the vapor phase in the 14 mm diameter orifice flow reactor. $ClONO_2$ (trace C) monitored at m/e 46 is amplified ten times during exposure time starting at t = 180 s. The observed reaction products are ICl (trace B), Cl_2 (trace A) and HOCl (trace D) monitored at m/e 162, 70 and 52, respectively. At t = 90 s the flow of $ClONO_2$ was halted before the plunger isolating the sample compartment was lifted, at t = 180 s the previous flow rate was reinstated. The lines guide the eye and represent an average through the data.

owing to the waning supply of HI at the interface. An additional contributing factor to increasing saturation could be the build-up of HNO_3, a primary reaction product which does not desorb from the ice under the present experimental conditions. However, this latter possibility is thought to be remote because to date no inhibiting effect of HNO_3 adsorbed onto ice has been found in heterogeneous reactions involving the mixed acid anhydrides $XONO_2$ and adsorbed hydrohalic acids HY.

No release of any of the expected product species into the gas phase is initially observed. Cl_2 which is the main product of the reaction appears after an induction time followed by a further delayed albeit transient release of ICl (see Fig. 2). When HOCl begins to appear the rate of formation of both Cl_2 and ICl have already peaked. The formation of Cl_2 is certainly due to the sequence of reactions (8), (9) and (1):

$$ICl + HI \rightarrow HCl + I_2 . \qquad (9, IH7)$$

Reaction (9) is apparently very efficient owing to the absence of any observable ICl at the beginning of the uptake experiment. This heterogeneous

Brought to you by | New York University Bobst Library Technical Services
Authenticated
Download Date | 7/25/15 6:50 AM

Table 3. Uptake and interfacial reactions of halogen compounds on ice and HX-doped ice measured in the 14 mm diameter orifice reactor at 200 K ("H"..halogen, "IH"..interhalogen reaction).

	Reaction	γ_0	Observations
H1	Br_2 + HBr	0.05±0.02	Seisel *et al.* [35] at T = 190 K
H2	I_2 on water ice	No uptake	Below detection limit
H3	I_2 + HCl	0.05±0.01	Reversible uptake
H4	I_2 + HBr	0.15±0.02	Reversible uptake
IH1	BrCl on water ice	No uptake	Interaction below detection limit
IH2	BrCl + HCl	0.045±0.010	No reaction observed
IH3	BrCl+HBr → HCl+Br_2	0.35±0.02	Reactive uptake: Immediate release of Br_2. HCl observed upon desorption.
		0.60±0.10	T = 190 K
IH4	ICl on water ice	0.09±0.02	Saturation. Reversible uptake
IH5	ICl + HCl	0.30±0.05	No reaction observed
IH6	ICl+HBr → HCl+IBr	0.30±0.02	Reactive uptake: HCl observed upon desorption. Strong negative temperature dependence (Fig. 5)
IH7	ICl+HI → HCl+I_2	0.32±0.02	Reactive uptake: HCl and I_2 observed upon desorption.
IH8	IBr on water ice	0.025±0.020	Instant saturation. Reversible uptake
IH9	IBr + HCl	0.20±0.05	No reaction observed
IH10	IBr + HBr	0.30±0.05	No reaction observed
IH11	IBr+HI → HBr+I_2	0.50±0.02	Reactive uptake: HBr and I_2 observed upon desorption

Brought to you by | New York University Bobst Library Technical Services
Authenticated
Download Date | 7/25/15 6:50 AM

reaction taking place on water-ice has indeed been experimentally studied and $\gamma = 0.13 \pm 0.02$ (reaction IH7 in Table 3) has been measured, as discussed below.

As a result of reaction (9) one would expect to observe I_2 in the gas phase as its interaction with ice (condensation/uptake) is very weak at this temperature. This has indeed been verified independently for pure ice (reaction H2 in Table 3). Yet in the presence of HCl non-reactive uptake of I_2 was taking place with $\gamma = 0.05 \pm 0.01$ according to reaction H3 (Table 3) implying that I_2 was effectively retained by the ice under the prevailing experimental conditions. By inference we argue that the same situation should hold even more so for the system I_2 + HI owing to the stability of the triiodide ion I_3^- so that one does not expect desorption of I_2 in the presence of either HCl, HBr or HI at low temperature. Consequently we believe that I_2 formed during the reaction sequence (8), (9) and (1) above remains trapped in the condensed phase owing most likely to the association of I_2 with I^{-1} resulting in the formation of the stable triiodide anion I_3^- [37]. The verification of this hypothesis may be obtained by using UV absorption spectroscopy in view of the large absorption coefficient of I_3^- of 2.3×10^4 and 3.8×10^4 l $mol^{-1}cm^{-1}$ at 352 and 290 nm, respectively [38−40]. If we assume these values to hold for I_3^- adsorbed onto ice at low temperature a formal monolayer of I_3^- based on a cross section of 43.4 $Å^2$ would result in an optical density leading to an absorption of 2% and 3.3% at 352 and 290 nm, respectively. However, these measurements would go beyond the scope of the present investigation.

C. $BrONO_2$ + HI/ice

The reaction of interest is displayed in reaction (10) with IBr as the expected primary reaction product:

$$BrONO_2 + HI \rightarrow IBr + HNO_3 . \quad (10)$$

For $BrONO_2$ interacting heterogeneously with HI-doped ice the situation is similar to reaction (8) involving $ClONO_2$ and results in an even larger uptake coefficient ($\gamma = 0.40 \pm 0.02$) at 200 K. A typical uptake experiment is displayed in Fig. 3 where the observed reaction products are IBr, Br_2 and HOBr monitored at m/e 206 (IBr^+), 160 (Br_2^+) and 98 ($HOBr^+$). Br_2 is observed as the main reaction product, resulting from the reaction sequence (10), (11) and (12). In contrast to reaction (8),

$$IBr + HI \rightarrow HBr + I_2 \quad (11), (IH11)$$

$$BrONO_2 + HBr \rightarrow Br_2 + HNO_3 \quad (12)$$

transient formation of IBr is observed without delay right after the start of the uptake experiment and HOBr begins to be formed once the HI supply at the interface has been depleted at t = 130 s (Fig. 3). Also, in contrast to

Brought to you by | New York University Bobst Library Technical Services
Authenticated
Download Date | 7/25/15 6:50 AM

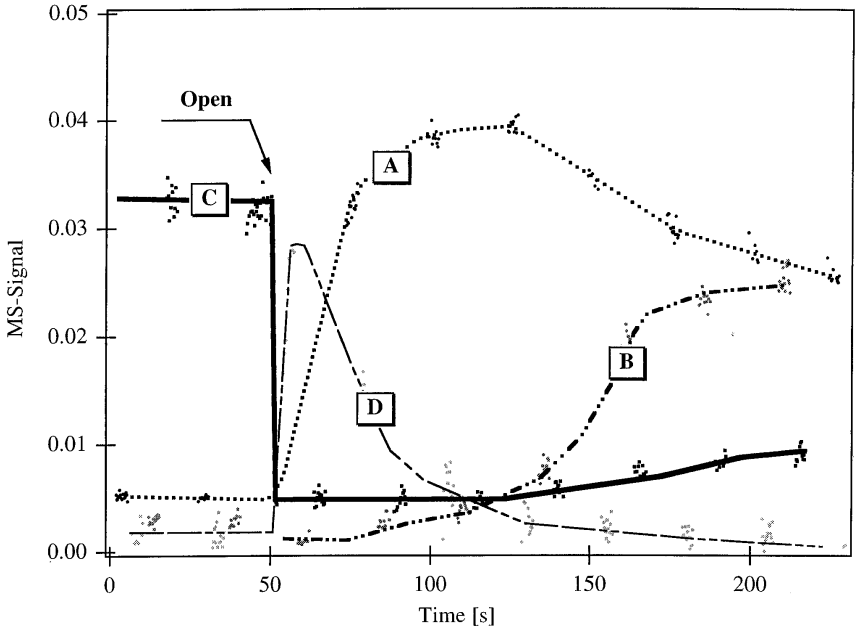

Fig. 3. The interaction of $BrONO_2$ with HI-doped ice condensed from the vapor phase in the 14 mm diameter orifice flow reactor. $BrONO_2$ (trace C) has been monitored at m/e 95. The observed reaction products are IBr (trace D), Br_2 (trace A) and HOBr (trace B) monitored at m/e 206, 160 and 98, respectively. The lines guide the eye and represent an average through the data (dots).

reaction (8) as well, the appearance of the expected primary product IBr precedes the observation of Br_2 which results from the fast secondary reaction (12). The rapid onset of IBr presented in Fig. 3 suggests that reaction (11) should be slower than reaction (9) under the given experimental conditions in order to allow the build-up of IBr which subsequently may desorb. However, this expectation does not match with the results of the reference experiments presented below, in which authentic samples of gas phase ICl and IBr heterogeneously interact with HI, the latter reacting almost twice as fast with HI compared to ICl (see Table 3, reactions IH7 and IH11 and Fig. 4). However, the actual reaction environment may be more complex than the experimental situation encountered in the reference experiment in which HNO_3 is absent and where the interhalogen (IBr) interacts from the gas phase with the substrate. Reaction (12) has been studied recently in which Br_2 has indeed been found as the major reaction product and $\gamma = 0.40 \pm 0.05$ has been measured [41].

The major difference between the $ClONO_2$/HI, reaction (8), and the $BrONO_2$/HI system, reaction (10), lies in the response time of the appear-

Brought to you by | New York University Bobst Library Technical Services
Authenticated
Download Date | 7/25/15 6:50 AM

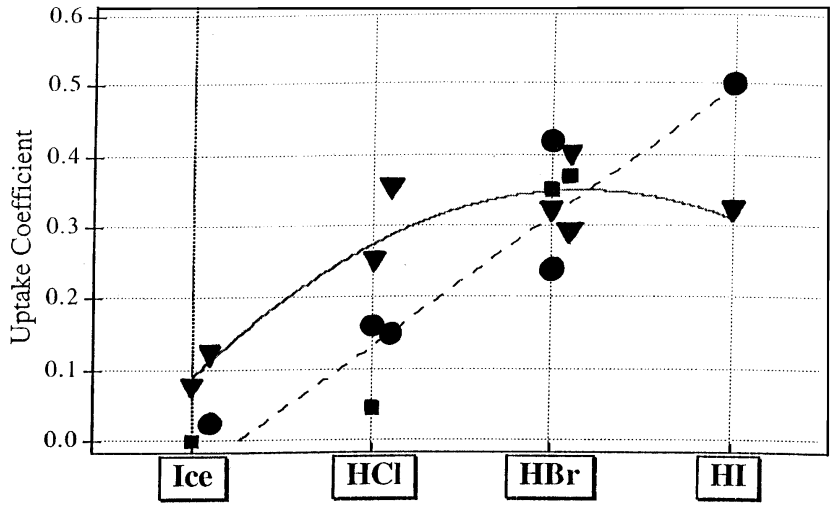

Fig. 4. Synposis of initial uptake coefficients γ_0 for the interaction of ICl (triangles), IBr (circles) and BrCl (squares) on HX-doped ice condensed from the vapor phase at 180 K and measured in the 14 mm diameter orifice flow reactor at 200 K under conditions of adding an external balancing H_2O flow in order to prevent evaporation of ice.

ance of the reaction products: the observation of both Cl_2 and ICl were delayed for reaction (8), while for reaction (10) the expected product IBr appears promptly as a transient followed by Br_2. The experiment displayed in Fig. 3 suggests that Br_2 results from the consumption of IBr formed in reaction (10) according to reaction (11), whereas ICl generated in reaction (8) appears once the supply of HI is starting to wane (Fig. 2). These experiments provide interesting information about the mechanism which appears to be complex and seems to be pointing towards different kinetics for key reactions (9) and (11). In addition, the presence of the other primary product, HNO_3, on the ice surface may prove to be a crucial factor for the reactions kinetics and the sequence of appearance of both primary and secondary reaction products. However, in contrast to reaction (1) HNO_3 did not show any inhibiting effect on an effective bimolecular reaction involving $BrONO_2$, for example in the reaction $BrONO_2$ + HCl [14].

D. The reactivity of the interhalogens BrCl, ICl and IBr on HX/ice (X = Cl, Br, I)

Considering the reaction mechanism of the foregoing three examples dealing with some of the heavier halogen analogs of the key heterogeneous reaction (1) of atmospheric importance it is evident that the complications arise from the occurrence of fast secondary reactions of the expected pri-

Brought to you by | New York University Bobst Library Technical Services
Authenticated
Download Date | 7/25/15 6:50 AM

mary reaction products, either halogens nearer than Cl_2 or interhalogens involving one halogen heavier than Cl. The kinetics of many of these secondary reactions of the type YZ + HX leading to halogen exchange are in many cases as fast as the reaction of interest so that the experimental separation of the different reactions becomes difficult, if not impossible. In retrospect, of all possible $YONO_2$ + HX only reaction (1) follows a simple, therefore direct mechanism as the primary reaction product Cl_2 has no measurable interaction with HCl under our experimental conditions of temperature and residence time. Although the existence of Cl_3^- is an experimentally proven fact [42], its stability against redissociation is very small [43]. In anticipation of the results on the halogen exchange reactions to be discussed we may state that there is a propensity of the $XONO_2$ + HY heterogeneous reaction to form the homonuclear halogen molecule owing to fast secondary halogen exchange reactions which are controlled by the thermodynamic stability of the final reaction products and whose mechanism most probably involves stable trihalogenide ions.

The experiments have been performed as follows: HX was first deposited on the ice sample at 200 K at a quantity of typically 20 monolayers. This means that at least for HCl the state of the HX/ice interface corresponded to a concentrated aqueous solution of HX located atop the bulk ice substrate. Subsequently, the HX-doped ice was exposed to a measured YZ flow and the rate of uptake as well as the reaction products were recorded. Eventually, the ice sample was heated so that adsorbed reaction products were thermally desorbed and all products could be quantitatively determined in order to establish a mass balance. The results are summarized in Table 3 and Fig. 4 below inasmuch as uptake coefficients γ and reaction products are concerned. No partial pressure dependence of γ has been experimentally measured.

At a low partial pressure of I_2 of approximately 10^{10} molecules cm^{-3} no uptake on ice is observed at 200 K. However, the situation changes substantially when HCl or HBr is present at the ice interface. In this case I_2 is actually taken up already at 200 K in a non-reactive manner in the following way:

$$I_2 + HCl \rightarrow H^+I_2Cl^- \quad (13)$$

$$I_2 + HBr \rightarrow H^+I_2Br^- \quad (14)$$

Although we have not examined the condensed phase for the presence of the trihalide ion the hypothesis of its formation is consistent with all observations made at the low temperature of approximately 200 K. The possibility of the detection of adsorbed I_3^- on ice using UV absorption spectroscopy has been discussed above.

Four cases of observed reactive uptake are displayed in Table 3, namely reactions IH3, IH6, IH7 and IH11 with confirmed reaction products observed after thermal desorption. In all cases it seems that the reaction is

Brought to you by | New York University Bobst Library Technical Services
Authenticated
Download Date | 7/25/15 6:50 AM

driven by the possibility to form the most stable hydrohalic acid (anion) like HCl (Cl^-) and HBr (Br^-) from iodine- and bromine-containing interhalogen compounds resulting in HCl (Cl^-), reactions (IH3), (IH6) and (IH7), and HBr (Br^-), reaction (IH11). The exothermicity of the halogen exchange reactions ($Y^- \Leftrightarrow X^-$) where Y is the heavier halogen atom scales with the difference in electronegativities. This is consistent with the results displayed in Table 3.

The interaction of I_2, BrCl, ICl and IBr with pure water ice, reactions (H2), (IH1), (IH4) and (IH8) in Table 3 does not scale with the molecular bond strength, namely 36 kcal mol^{-1}, 52 kcal mol^{-1}, 51 kcal mol^{-1} and 43 kcal mol^{-1}, respectively, which seems to suggest that it is ionic in nature. The coefficient γ for uptake on ice is highest for ICl (0.09 ± 0.023) which has the highest difference in electronegativity ΔEN of the atoms and has therefore the highest dipole moment of all interhalogen compounds investigated. The uptake coefficient γ is approximately a factor of four lower for IBr (0.025 ± 0.010) in relation to ICl, whereas it vanishes for both BrCl and I_2. Instead, the trend in the uptake rate as given by γ seems to scale with the dipole moments whose sequence is expected to decrease in the series ICl > IBr > BrCl > I_2 according to the known value of ΔEN. This indicates the importance of the polarity of the molecule in its interaction with the ice matrix caused by electronegativity differences ΔEN in the isolated interhalogen species and the dipole-dipole interactions once it starts to interact with the ice substrate.

On HX-doped ice we observe a generally increasing trend of γ with increasing molecular weight of HX (see Fig. 4). The only exception to this series is the interaction of ICl with HI which seems to be approximately a factor of two smaller than expected (see Table 3). In fact, γ seems to reach an upper limit of 0.30 ± 0.05 for all the HX reactions involving ICl. Apparently, this behavior is opposite to the one observed for IBr, whose γ value increases in the series HCl < HBr < HI/ice as displayed in Fig. 4, and for BrCl whose γ value is larger for HBr than for HCl/ice. These observed trends compare rather well with the results obtained by Wang [44] and Troy [37] in aqueous solutions from a qualitative point of view. These authors investigated the interaction of ICl and IBr with I^- and proposed the mechanism displayed in reactions (15) and (16) with (X = Cl, Br) which accounts for the products we detected upon desorption for reactions (IH7) and (IH11) listed in Table 3.

$$IX + I^- \Leftrightarrow I_2X^- \tag{15}$$

$$I_2X^- \Leftrightarrow I_2 + X^- \tag{16}$$

In an analogous manner we propose the following equilibrium for reactions (IH5) and (IH10) which corresponds to a non-reactive case because the reactant is already the most stable hydrohalic acid:

$$IX + X^- \Leftrightarrow IX_2^- \,. \tag{17}$$

Brought to you by | New York University Bobst Library Technical Services
Authenticated
Download Date | 7/25/15 6:50 AM

Ab initio calculations performed for reaction (IH7) and (IH11) in solution albeit at room temperature [45] indicate that IX_2^- is stabilized as $(X\text{-}I\text{-}X)^-$ at the interface, with the heavier atom in the center of the trihalide anion. In the case of the present experiments where IX has been exposed to HX-doped ice, thermal desorption displaces the equilibrium to the left of reaction (17) and regenerates the initial reactants for reactions (IH5) and (IH10).

For reaction (IH6) and its reverse, reaction (IH9), our observations point towards the following mechanism (Y = Cl, X = Br for (IH6) and vice versa for (IH9)):

$$IX + Y^- \Leftrightarrow YIX^- \quad \text{with } YIX^- = BrICl^- \tag{18}$$

$$BrICl^- \Leftrightarrow IBr + Cl^- . \tag{19}$$

This explains the apparent non-reactive character of reaction (IH9) as opposed to reaction (IH6) because in the former HCl already represents the most stable hydrohalic acid relative to HBr. The formation of the chloride ion is energetically favored because of the higher electron affinity of the Cl atom (83.2 kcal mol^{-1}) compared to Br atom (77.4 kcal mol^{-1}) [46].

Reaction (IH2) leads to the formation of $BrCl_2^-$ which is most probably stabilized as $(Cl\text{-}Br\text{-}Cl)^-$ at the interface in analogy to the molecular structures involving iodine as a central atom [45]:

$$BrCl + Cl^- \Leftrightarrow BrCl_2^- . \tag{20}$$

The experimental equilibrium constant obtained for reaction (20) in solution is almost an order of magnitude lower than that measured for reaction (17) between ICl and Cl^- with $X = Cl^-$ [42, 44], indicating that $BrCl_2^-$ is prone to redissociation compared to ICl_2^-, hence the lower uptake coefficients measured in this study for reaction (IH2). One has to remember that the uptake measurement refers to the net effect of combined adsorption and desorption rate.

Our experimental observations concerning reaction (IH3) point towards the following scheme:

$$BrCl + Br^- \Leftrightarrow Br_2Cl^- \tag{21}$$

$$Br_2Cl^- \Leftrightarrow Br_2 + Cl^- \tag{22}$$

In this case as well the halogen exchange takes place resulting in the substitution of the thermodynamically more favored Cl^- compared to Br^- as the hydrated ionic species. The measured value of the uptake coefficient is significantly higher for reaction (IH3) than for reaction (IH2), thus pointing to the higher stability of the intermediate $(Br\text{-}Br\text{-}Cl)^-$ compared to $(Br\text{-}Cl\text{-}Cl)^-$, in agreement with previous experimental and theoretical studies [42–45].

In addition, the concept of trihalide ion formation has also been invoked in the discussion of the interfacial kinetics of Cl_2 on I^- and Br^--containing

Brought to you by | New York University Bobst Library Technical Services
Authenticated
Download Date | 7/25/15 6:50 AM

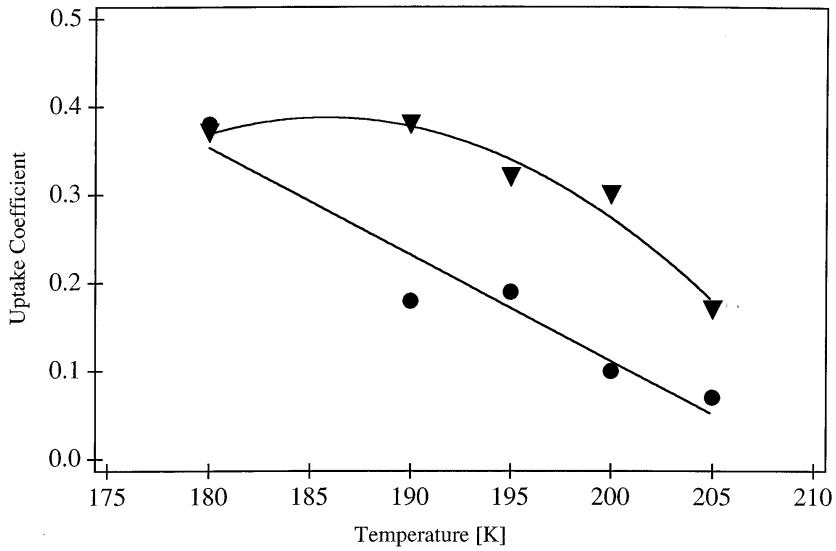

Fig. 5. The temperature dependence of the initial uptake coefficient γ_0 for the interaction of ICl on ice condensed from the vapor phase at T = 180 K and on ice doped with approximately ten formal monolayers of HBr measured in the 14 mm diameter orifice flow reactor: ICl/ice (circles), ICl/HBr-doped ice (triangles).

solutions as well as of Br_2 interacting with I^--containing solutions. Because the solubility of Cl_2 and Br_2 is low interfacial effects are given the chance to play a role, especially when there is a tendency to form a stable trihalide complex in solution [27].

By varying the temperature from 180 K to 205 K for the reaction of ICl with adsorbed HBr, reaction (IH6), we observed a significant negative temperature dependence in agreement with the proposal for the formation of a trihalide complex $BrICl^-$ located at the interface (Fig. 5, triangles). An Arrhenius plot obtains an activation energy of $E_a = -5.0 \pm 2.0$ kcal/mol if we exclude the γ value at the lowest temperature of 180 K. This last point suggests that the negative temperature dependence flattens out towards lower temperatures as has been observed in the past [47], presumably owing to a change in the reaction mechanism. The uptake of ICl on ice saturates after a few seconds and is reversible. Therefore, the values displayed in Fig. 5 (circles) correspond to the initial uptake coefficient γ_0 whose temperature dependence yields an activation energy of $E_a = -5.8 \pm 2.0$ kcal/mol. The uptake of ICl on HBr-doped ice, on the other hand, is reactive and does not saturate as it is sustained until exhaustion of the supply of HBr at the interface. A strong negative temperature dependence has also been observed for reaction (IH3) leading to the unstable trihalide ion $(Cl\text{-}Br\text{-}Br)^-$. We take

Brought to you by | New York University Bobst Library Technical Services
Authenticated
Download Date | 7/25/15 6:50 AM

the negative temperature dependence of γ, albeit over a very limited temperature range, as a strong indication for the validity of the trihalide ion hypothesis.

4. Atmospheric relevance

The present work has been undertaken with the goal to study the rate of uptake on frozen surfaces containing H_2O as well as to unravel the reaction mechanism at the temperature of interest. We do not claim to have studied these reactions under stratospheric conditions because the partial pressures of $ClONO_2$ and $BrONO_2$ used in our study are approximately 2 to 3 orders of magnitude larger than in the stratosphere. However, we may assert that both the uptake kinetics (γ) as well as the product spectrum may be valid even under stratospheric conditions because we did not observe any significant partial pressure dependence of γ indicating the absence of major saturation effects under the present experimental conditions.

In essence, all three of the halogen nitrate reactions examined in the present work are fast spanning the range of γ between 0.3 and 0.6 at 200 K akin to the often examined reaction (1). However, the noted propensity for the formation of the homonuclear halogen molecule is unexpected and is the result of fast secondary reactions involving the primary interhalogen product which have been examined in the second part of this work. In a reaction of the type

$$YONO_2 + HX_{(ads)} \rightarrow XY + HNO_{3(ads)} \tag{23}$$

the ensuing fast secondary reaction may proceed according to reaction (24) or (25) depending on whether it belongs to the non-reactive (24) or reactive (25) type:

$$HX_{(ads)} + XY \Leftrightarrow H^+(X_2Y)^- \tag{24}$$

$$HX_{(ads)} + XY \rightarrow HY_{(ads)} + X_2\,. \tag{25}$$

In the latter case, into which all three reactions studied in this work fall, an additional reaction channel (26) may be active once a sufficient quantity of HY has accumulated at the interface:

$$YONO_2 + HY_{(ads)} \rightarrow Y_2 + HNO_{3(ads)}\,. \tag{26}$$

It may be seen that the net result is either formation of the homonuclear halogen species X_2 or Y_2 in reaction (25) and (26) or the build-up of a reservoir trihalide anion $(X_2Y)^-$ in reaction (24). In this latter case the primary product XY is involved in a reversible equilibrium whose stability constant favours the right-hand side of reaction (24). With decreasing stability of $(X_2Y)^-$ the primary product XY is released into the gas phase such as for instance in the case of the reaction $BrONO_2$ + HCl on ice in the range 180−200 K [14]. In short, the essential reason for the propensity to

Brought to you by | New York University Bobst Library Technical Services
Authenticated
Download Date | 7/25/15 6:50 AM

form homonuclear halogen species resulting from the above reactions is the tendency for the formation of trihalide anions with the minimum requirement that at least one atom must be a Br or a heavier halogen. This may be seen in the lightest example $(BrCl_2)^-$ whose formation on HCl-doped ice is supported by our measurements, reaction (IH2) (see Table 3).

It is interesting to note that Spicer *et al.* [48] have recently detected significant amounts of night-time Cl_2 in the marine boundary layer. Although its origin has by no means been elucidated and probably lies in a reaction such as HOCl or $ClONO_2 + Cl^-$ in or on liquid marine aerosols, the results of this work may indicate that the formation of molecular halogens in the atmosphere could be more widespread than previously thought.

Acknowledgement

Funding for this work has been generously provided by the Office Fédéral de l'éducation et de la science (OFES) in the framework of the subproject LEXIS of the EU program "Environment and Climate".

References

1. S. Solomon, R. R. Garcia, F. S. Rowland and D. J. Wuebbles, Nature **321** (1986) 759.
2. M. J. Molina, in *The Chemistry of the Atmosphere: Its impact on Global Change*, B. J. Calvert (ed.), 1994, Oxford, United Kingdom.
3. Scientific Assessment of Ozone Depletion: 1998, World Meteorological Organization Global Ozone Research and Monitoring Project, Report No. 44, Global Ozone Observing System (GO_3OS).
4. R. Oppliger, A. Allanic and M. J. Rossi, J. Phys. Chem. **101** (1997) 1903.
5. L. Barrie and U. Platt, Tellus **49B** (1997) 450.
6. I. G. Nolt, P. A. R. Ade, F. Alboni, B. Carli, M. Carlotti, U. Cortesi, M. Epifani, M. J. Griffin, P. A. Hamilton, C. Lee, G. Lepri, F. Mancaraglia, A. G. Murray, J. H. Park, K. Park, P. Raspolini, M. Ridolfi and M. D. Vanek, Geophys. Res. Lett. **24** (1997) 281.
7. J. G. Anderson, W. H. Brune, S. A. Lloyd, D. W. Toohey, S. P. Sander, W. L. Starr, M. Loewenstein and J. R. Podolske, J. Geophys. Res. **94** (1989) 11480.
8. K. A. McKinney, J. M. Pierson and D. W. Toohey, Geophys. Res. Lett. **24** (1997) 853.
9. C. T. McElroy, C. A. McLinden and J. C. McConnell, Nature **397** (1999) 338.
10. T. Wagner and U. Platt, Nature **395** (1998) 486.
11. K. Hebestreit, J. Stutz, D. Rosen, V. Matveiv, M. Peleg, M. Luria and U. Platt, Science **283** (1999) 55.
12. J. B. Burkholder, A. R. Ravishankara and S. Solomon, J. Geophys. Res. **100** (1995) 16793.
13. D. R. Hanson and A. R. Ravishankara, "Reaction of halogen species on ice surfaces", in *The Tropospheric Chemistry of Ozone in the Polar Regions*, edited by H. Niki and K. H. Becker, NATO ASI Ser., Springer Verlag, New York, Berlin **17** (1993) 281.
14. A. Allanic, R. Oppliger and M. J. Rossi, J. Geophys. Res. **102** (1997) 23529.
15. W. L. Chameides and D. D. Davis, J. Geophys. Res. **85** (1980) 7383.
16. R. B. Chatfield and P. J. Crutzen, J. Geophys. Res. **95** (1990) 22319.

Brought to you by | New York University Bobst Library Technical Services
Authenticated
Download Date | 7/25/15 6:50 AM

17. M. E. Jenkin, "A comparative assessment of the role of iodine photochemistry in tropospheric ozone depletion", in *The Tropospheric Chemistry of Ozone in the Polar Regions*, edited by H. Niki and K. H. Becker, NATO ASI Ser., Springer Verlag, New York, Berlin **17** (1993) 405.
18. S. Solomon, R. R. Garcia and A. R. Ravishankara, J. Geophys. Res. **99** (1994) 20491.
19. D. Davis, J. Crawford, S. Kiu, S. McKeen, A. Bandy, D. Thornton, F. Rowland and D. Blake, J. Geophys. Res. **101** (1996) 2135.
20. L. J. Carpenter, W. T. Sturges, S. A. Penkett, P. S. Liss, B. Alicke, K. Hebestreit and U. Platt, J. Geophys. Res. **104** (1999) 1679.
21. B. Flückiger, A. Thielmann, L. Gutzwiller and M. J. Rossi, Ber. Bunsenges. Phys. Chem. **102** (1998) 915.
22. A. Allanic and M. J. Rossi, J. Geophys. Res. **104** (1999) 18689.
23. P. Campuzano-Jost and J. N. Crowley, J. Phys. Chem. **103** (1999) 2712.
24. M. B. McElroy, R. J. Salawitch, S. C. Wofsy and J. A. Logan, Nature **321** (1986) 759.
25. A. B. Horn, J. R. Sodeau, T. B. Roddis and N. A. Williams, J. Phys. Chem. **102** (1998) 6107.
26. J. P. McNamara, G. Tresadern and I. H. Hillier, Chem. Phys. Lett. **310** (1999) 265.
27. J. H. Hu, Q. Shi, P. Davidovits, D. R. Worsnop, M. S. Zahniser and C. E. Kolb, J. Phys. Chem. **99** (1995) 8768.
28. C. E. Kolb, D. R. Worsnop, M. S. Zahniser, P. Davidovits, L. F. Keyser, M.-T. Leu, M. J. Molina, D. R. Hanson, A. R. Ravishankara, L. R. Williams and M. A. Tolbert, Laboratory Studies of Atmospheric Heterogeneous Chemistry, in *Progress and Problems in Atmospheric Chemistry*, (J. R. Barker, ed.), Adv. Ser. Phys. Chem. **vol. 3**, 771, World Sci., River Edge, N.J., 1995.
29. F. Caloz, F. F. Fenter, K. D. Tabor and M. J. Rossi, Rev. Sci. Instrum. **68** (1997) 3172.
30. F. F. Fenter, F. Caloz and M. J. Rossi, Rev. Sci. Instrum. **68** (1997) 3180.
31. R. S. Timonen, L. T. Chu, M. T. Lu and L. F. Keyser, J. Phys. Chem. **98** (1994) 9509.
32. W. W. Wilson and K. O. Christe, Inorg. Chem. **26** (1987) 1573.
33. D. R. Stull and C. B. Prophet, JANAF Thermodynamical Tables, Publication NSRDS-NBS 37, 1971.
34. Evaluated Kinetic and Photochemical Data for Atmospheric Chemistry. Supplement V. IUPAC Subcommittee on Gas Kinetic Data Evaluation for Atmospheric Chemistry, R. Atkinson, D. L. Baulch, R. A. Cox, R. F. Hampson, Jr., J. A. Kerr (Chairman), M. J. Rossi and J. Troe, J. Phys. Chem. Ref. Data **26** (1997) 509−1011.
35. S. Seisel, B. Flückiger and M. J. Rossi, Ber. Bunsenges. Phys. Chem. **102** (1998) 811.
36. S. Seisel and M. J. Rossi, Ber. Bunsenges. Phys. Chem. **101** (1997) 943.
37. R. C. Troy, M. D. Kelley, J. C. Nagy and D. W. Margerum, Inorg. Chem. **30** (1991) 4838.
38. W. Gabes and D. J. Stufkens, Spectrochim. Acta A **30** (1974) 1835.
39. M. Mizuno, J. Tanaka and I. Harada, J. Phys. Chem. **85** (1981) 1789.
40. T. Okada and J. Hata, Mol. Phys. **43** (1981) 1151.
41. A. Aguzzi and M. J. Rossi, in preparation.
42. T. X. Wang, M. D. Kelley, J. N. Cooper, R. C. Beckwith and D. W. Margerum, Inorg. Chem. **33** (1994) 5872.
43. Y. Ogawa, O. Takahashi and O. Kikuchi, J. Mol. Struct. **424** (1998) 285.
44. Y. L. Wang, J. C. Nagy and D. W. Margerum, J. Am. Chem. Soc. **111** (1989) 7838.
45. Y. Ogawa, O. Takahashi and O. Kikuchi, J. Mol. Struct, **429** (1998) 187.
46. H. M. Rosenstock, K. Draxl, B. W. Steiner and J. T. Herron, Energetic of gaseous ions, Journal of physical and chemical reference data **6** (1977) Suppl. 1.
47. L. Chaix, H. van den Bergh and M. J. Rossi, J. Phys. Chem. **102** (1998) 10300.
48. C. W. Spicer, E. G. Chapman, B. J. Finlayson-Pitts, R. A. Plastridge, J. M. Hubbe, J. D. Fast and C. M. Berkowitz, Nature **394** (1998) 353.

Brought to you by | New York University Bobst Library Technical Services
Authenticated
Download Date | 7/25/15 6:50 AM